

# $^{31}\text{P}$ magnetic resonance spectroscopy of the breast and the influence of the menstrual cycle

B. L. Stehouwer · W. J. M. van der Kemp ·  
P. R. Luijten · M. A. A. J. van den Bosch ·  
W. B. Veldhuis · J. P. Wijnen · D. W. J. Klomp

Received: 9 January 2014 / Accepted: 15 February 2014 / Published online: 26 February 2014  
© Springer Science+Business Media New York 2014

**Abstract** Phosphorus metabolite ratios are potential biomarkers in breast cancer diagnosis and treatment monitoring. Our purpose was to investigate the metabolite ratios phosphomonoester to phosphodiester, phosphoethanolamine (PE) to glycerophosphoethanolamine (GPE), and phosphocholine (PC) to glycerophosphocholine (GPC) in glandular breast tissue, and the potential effect of the menstrual cycle, using  $^{31}\text{P}$  magnetic resonance spectroscopy (MRS) at 7T. Seven women with regular menstrual cycles each underwent four examinations using a 3D  $^{31}\text{P}$  multi-echo magnetic resonance spectroscopic imaging sequence. Peak integrals were assessed using IDL and JMRUI software. First, T2 relaxation times were calculated using multi-echo data pooled across subjects and time points. Subsequent, metabolite ratios were calculated for each phase of the menstrual cycle using the calculated T2 values to account for when combining the free induction decay and all five echoes. The metabolite ratios were calculated both on group level and individually. T2 decay fits resulted in a T2 relaxation time for PE of 154 ms (95 % CI 144–164), for PC of 173 ms (95 % CI 148–205), for Pi of 188 ms (95 % CI 182–193), for GPE of 48 ms (95 % CI 44–53), and for GPC of 23 ms (95 % CI 21–26). The metabolite ratios analyzed on group level showed negligible variation throughout the menstrual cycle. Individual results did show an apparent intra-individual variation; however, not significant due to the measurements' uncertainty. To conclude, phospholipids in glandular tissue as

measured with  $^{31}\text{P}$  MRS at 7 T are not significantly affected by the menstrual cycle.

**Keywords**  $^{31}\text{P}$  MRS · Breast · Menstrual cycle · Glandular tissue

## Abbreviations

DCE	Dynamic contrast-enhanced
tCho	Total pool of choline and ethanolamine containing compounds resonating around 3.2 ppm
PME	Phosphomonoesters
PC	Phosphocholine
PE	Phosphoethanolamine
PDE	Phosphodiesters
GPC	Glycerophosphocholine
GPE	Glycerophosphoethanolamine
EF	Early follicular phase
LF	Late follicular phase
EL	Early luteal phase
LL	Late luteal phase
Pi	Inorganic phosphate
PCr	Phosphocreatine

## Introduction

Breast cancer is the most common malignancy in women worldwide [1]. Radiological imaging is essential in the patients work-up to establish a diagnosis and to determine a treatment plan. Dynamic contrast-enhanced (DCE) MRI is regularly used in the evaluation of breast lesions as well as for the monitoring of patients who receive neoadjuvant chemotherapy [2, 3]. Although DCE breast MRI has a high sensitivity for the detection of breast lesions, the specificity is relatively low; approximately 70 % [4]. The same

B. L. Stehouwer (✉) · W. J. M. van der Kemp ·  
P. R. Luijten · M. A. A. J. van den Bosch ·  
W. B. Veldhuis · J. P. Wijnen · D. W. J. Klomp  
Department of Radiology, University Medical Center Utrecht,  
Room E01.132, PO Box 85500, 3508 GA Utrecht, Netherlands  
e-mail: B.L.Stehouwer@umcutrecht.nl

accounts for the effectiveness of DCE MRI in treatment monitoring, which has shown to be variable depending on receptor status of the tumor [5]. Therefore, other techniques are investigated to improve specificity.

One of the techniques of interest is MR Spectroscopy (MRS) or MR Spectroscopic Imaging (MRSI). With MRS(I) metabolites can be measured noninvasively. To date, patient studies mainly focused on proton ( $^1\text{H}$ ) MRS [6].  $^1\text{H}$  MRS levels of the total pool of choline and ethanolamine containing compounds resonating at 3.2 ppm (tCho) are measured to evaluate the presence of malignancy and its response to therapy [6–8]. However, tCho contains multiple different metabolites that individually play a role in the tumor metabolism [9]. With phosphorus ( $^{31}\text{P}$ ) MRS the phosphomonoesters (PME): phosphocholine (PC) and phosphoethanolamine (PE), as well as the phosphodiester (PDE): glycerophosphocholine (GPC) and glycerophosphoethanolamine (GPE), can be measured individually, which was shown for the first time in breast cancer patients in 1988 [10]. Elevated PME to PDE levels have been associated with the presence of cancer, while a fall in PME to PDE levels is seen in case of effective therapy [11]. Other *ex vivo* work described a lower PC to GPC ratio to be indicative of more aggressive breast cancer subtypes, such as triple negative breast cancer [12]. Since phosphorus is less abundant than protons in the human body, and the gyromagnetic constant of  $^{31}\text{P}$  is a factor 2.5 lower than that of  $^1\text{H}$ , the measurements are challenging due to a lack of signal-to-noise ratio (SNR). However, recent studies have shown that  $^{31}\text{P}$  MRS(I) at 7.0 Tesla (7 T) is feasible for *in vivo* detection and quantification of phosphorus metabolites [13, 14] with acceptable acquisition times and sufficient spatial resolution, particularly when using multi-echo acquisitions [15].

It is well known that, due to hormonal fluctuations, breast tissue changes during the menstrual cycle [16, 17]. Research has been performed to evaluate in which phase of the menstrual cycle DCE MRI should preferably be performed to avoid false positive readings due to contrast agent uptake in normal glandular tissue [18–21]. However, there is only little data on normal values of phosphorus metabolites and their fluctuation during all phases of the menstrual cycle measured with  $^{31}\text{P}$  MRS. Consequently, it is unclear whether it can be combined with DCE MRI in clinical practice at the optimal timing for both methods. Of the published data, one study, performed in four premenopausal women at a compromised SNR at 1.5 T, does suggest that the PME, PDE, and total  $^{31}\text{P}$  signals change during the menstrual cycle [22]. A second study, including five premenopausal women who were not taking oral contraceptives scanned at 1.5 T as well, found a significant lower PME relative peak area in second week of the menstrual cycle as well as a significant higher PDE/PME peak area ratio [23].

Knowledge of normal values, and their fluctuation during the menstrual cycle, offers a framework for the interpretation of breast cancer patient data. Therefore, in this study, we investigated the phospholipid metabolism in glandular breast tissue and the influence of the menstrual cycle on the metabolism with  $^{31}\text{P}$  MRS at 7 T.

## Methods

### Subjects and data acquisition

Seven female volunteers were included who had a regular menstrual cycle and did not use any hormonal contraceptives. The mean age was 27 years (range 24–30 years). Each volunteer underwent four 7 T MRSI examinations, one in each phase of the menstrual cycle: the early follicular phase (EF), late follicular phase (LF), early luteal phase (EL), and late luteal phase (LL), resulting in 28 examinations in total. Before each examination the menstrual cycle status was reported and informed consent was signed. All examinations were performed in compliance with the local institutional ethics committee.

The examinations were performed on a 7 T whole-body scanner (Philips Healthcare, Cleveland, OH, USA) using a two-channel double-tuned unilateral RF breast coil (MR Coils BV, Drunen, the Netherlands), with the resonance frequencies of 298 and 121 MHz for  $^1\text{H}$  and  $^{31}\text{P}$ , respectively [13, 24]. All volunteers were scanned in prone position with the coil encompassing the right breast. The scan protocol consisted of a 3D T1w sequence [TR/TE 4.0/2.0 ms, binomial flip angle  $5^\circ$ , FOV  $160 \times 160 \times 160 \text{ mm}^3$ , acquired resolution  $1 \times 1 \times 2 \text{ mm}^3$ ], and a 3D  $^{31}\text{P}$  multi-echo MRSI sequence, using spherical k-space sampling and an excitation bandwidth of 800 Hz [TR/TE 6000/45 ms, adiabatic flip angle  $90^\circ$ , FOV  $320 \times 160 \times 320 \text{ mm}^3$ , nominal spatial resolution  $40 \times 20 \times 40 \text{ mm}^3$ ]. One free induction decay (FID) and 5 full echoes were acquired within one TR, resulting in the five echoes being at 45, 90, 135, 180, and 225 ms, respectively. Both the FID and echoes were acquired with 256 data points. The MRS sequence is described in more detail elsewhere [15]. Total scanning time was approximately 30 min.

### Data analysis

The spectroscopy data were analyzed using IDL (Research Systems, Boulder, CO) and JMRUI 4.0 software [25]. Acquired data were Hamming filtered in the spatial domain and zero-filled to 8,192 data points in the time domain. The hamming filtering resulted in voxels with an elliptical full-width half-max of  $68 \times 34 \times 68 \text{ mm}^3$ . One localized voxel from the MRSI examination containing glandular

tissue, represented by high inorganic phosphate (Pi) and low phosphocreatine (PCr) signal, was chosen to use in the analyses. For each volunteer's examination the optimal voxel was chosen, which could be the same or a different voxel at each of the four time points. All spectra, i.e., FIDs and echoes, were frequency aligned to Pi. Subsequently, all spectra were summed for the FID and each of the five echoes separately within JMRUI, weighted by the Pi signal for the FID. Metabolite quantification for PC, PE, GPE, and GPC was done in JMRUI using the AMARES algorithm on the summed spectra [26]. Prior to metabolite quantification, the average value of chemical shifts of all metabolites in each sum spectrum (1 sum total FID and 5 sum total echo spectra) was determined. Furthermore, the sum spectra were apodized with 40 Hz, representing the smallest line width found. During quantification the line widths of PE, PC, GPE, and GPC were set equal in each sum spectrum. The line widths determined for phosphomono- and phosphodiesteres of the different sum spectra ranged between 56 and 67 Hz, for Pi the linewidth ranged between 45 and 55 Hz for the different sum spectra. The difference in range corresponds to peak broadening for PME and PDE caused by  $^1\text{H}$ - $^{31}\text{P}$  J-coupling. The chemical shift values used in the quantification were constrained to the average chemical shift values (over the 4 cycle points) with a soft constraint of  $\pm 0.05$  ppm. Overall phases were fixed to zero in the quantification.

The peak integrals for PE, PC, GPE, and GPC, obtained in the sum spectrum of all FIDs and in the sum spectrum of each echo, were used to calculate metabolite T2 values. Standard deviations of the T2 values were determined using Monte Carlo simulations, representing the uncertainty of the fittings. Metabolite ratios were determined based on the spectrum of the FID plus 5 echoes combined. The combining was performed accounting for the T2 relaxations times of the metabolites, where the full echoes were weighted two times in comparison to the FID. This resulted in a sum spectrum per metabolite which was used for quantification. The metabolite quantification was done on group level and for each volunteer separately. Standard deviations of the metabolite ratios were determined using

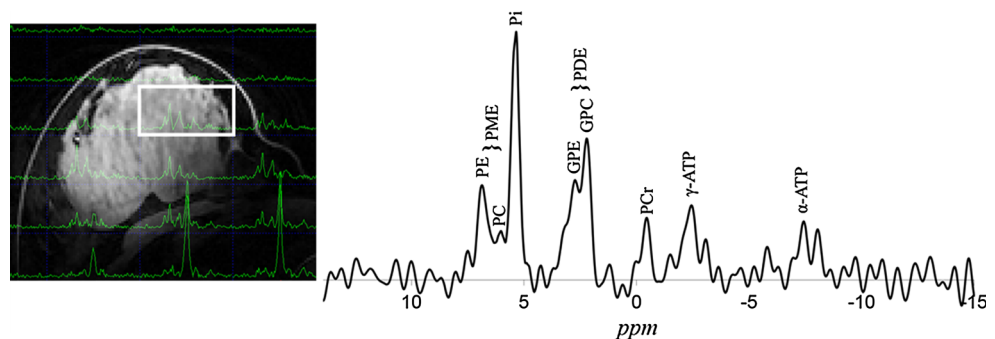
Monte Carlo simulations, representing the measurements uncertainty. All three metabolic ratios were tested for significant variation over the menstrual cycle on the individual data using Friedman's two-way ANOVA test.

## Results

All 28 examinations were conducted successfully. In the analysis first a voxel containing glandular tissue was chosen for each measurement. One example is presented in Fig. 1. A large proportion of the selected voxel in Fig. 1 contains glandular tissue while chest wall muscle was excluded, resulting in a high Pi signal and relatively low PCr, as can be seen in the spectrum. Of all measurements one did not show sufficient signal from phosphorus resonances ( $\text{SNR} < 3$ ), resulting in 27 exams to be included in the final analyses.

Second, the T2 relaxation times of the metabolites were calculated using the data of all volunteers combined for the FID and for each echo. These six pooled spectra (1 FID and 5 echoes) are shown in Fig. 2. It can be observed that the phosphomonoesters decay much slower than the phosphodiesteres. T2 decay plots were made for each of the metabolites, resulting in a T2 relaxation time for PE of 154 ms (95 % CI 144–164), for PC of 173 ms (95 % CI 148–205), for Pi of 188 ms (95 % CI 182–193), for GPE of 48 ms (95 % CI 44–53), and for GPC of 23 ms (95 % CI 21–26). Subsequently, the combined data of the FID and echoes were analyzed, on group basis and on individual basis, accounting for the calculated T2 relaxation times of the metabolites (i.e., the FID and echoes were T2-weighted and summed on a group level and individually). The phosphorus metabolite ratios of these spectra analyzed on group level are presented in Table 1 and Fig. 3.  $^{31}\text{P}$  MR spectra, analyzed on group level, in the four phases of the menstrual cycle are displayed in Fig. 4. The results for the seven volunteers individually are displayed in Fig. 3. In the group analysis a negligible variation in metabolic ratios throughout the menstrual cycle is observed, which is similar to the inaccuracy (expressed as standard deviations) of the measurement. The individually

**Fig. 1** T1w 3D FFE image with a representation of the grid of voxels and their spectra. The voxel selected for the analysis is highlighted, of which the  $^{31}\text{P}$  FID spectrum is shown. Note the relatively high PME, Pi, and PDE signals in contrast to the relatively low PCr signal in the spectrum of the selected voxel



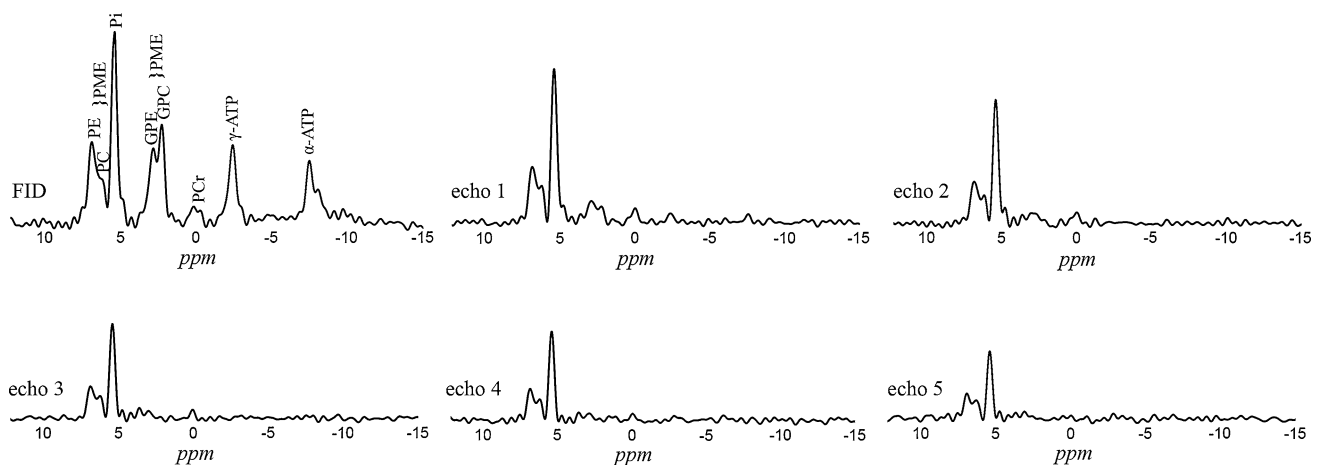


**Fig. 2**  $^{31}\text{P}$  MR spectra of the FID and five echoes using the data of all volunteers combined. From these spectra T2 fits were made for PE, PC, GPE, and GPC. Note the fast decay of PDE, and slower decay of PME

**Table 1** Metabolic ratios for the combined FID plus multi-echo data on group level, presented per phase of the menstrual cycle

Metabolic ratios of FID plus multi-echo data $\pm$ SD				
	EF	LF	EL	LL
PME/PDE	$0.75 \pm 0.02$	$0.70 \pm 0.02$	$0.69 \pm 0.03$	$0.72 \pm 0.02$
PE/GPE	$1.23 \pm 0.08$	$1.13 \pm 0.08$	$1.19 \pm 0.10$	$1.24 \pm 0.09$
PC/GPC	$0.40 \pm 0.04$	$0.36 \pm 0.03$	$0.33 \pm 0.04$	$0.37 \pm 0.03$

analyzed data show more variation between the volunteers as well as between phases in the menstrual cycle within the volunteers; however, the standard variations are larger as well. No specific pattern of variation during the menstrual cycle is observed for any of the ratios, and magnitudes of the observed variations are in the order of the experimental uncertainties ( $P = 0.86$ ,  $P = 0.90$ ,  $P = 0.75$ , for PME to PDE, PE to GPE, and PC to GPC, respectively).

## Discussion

In this study no significant variations in phosphorus metabolite ratios over the menstrual cycle were measured on group level using  $^{31}\text{P}$  MRS in the breast at 7 T. In the individual data analysis more variation was observed over the menstrual cycle intra-individually. However, the variation showed neither a specific pattern nor statistical significance since the measurements' uncertainty is greater than the observed variations.

In previous work, where  $^{31}\text{P}$  MRS was similarly assessed in four premenopausal women, the summed data showed PME to PDE ratios of 1.06, 1.75, 0.48, and 0.78 for EF, LF, EL, and LL, respectively [22]. In our study, the summed data showed PME to PDE ratios of 0.75, 0.70, 0.69, and 0.72, indicating a more stable course throughout

the menstrual cycle. Furthermore, the reported lower PME peak area in the late follicular phase—as measured in five women by Twelves et al. [23] was not reproduced, nor did we find significant lower levels of the individual monoesters PE and PC in any phase when assessing the metabolic ratios. In contrast to previous work, the SNR in our study was higher, which can be appreciated in the presented spectra. The higher SNR, and also higher spectral resolution provided by 7 T, allowed for assessment of the PE/GPE and PC/GPC ratio as well. Still, the measurements uncertainty, as can be observed by the standard deviations of the ratios, especially in the individual assessment, remains greater than the observed variation.

A relatively low PCr signal can be observed in the presented spectra. PCr has been reported to originate mainly from the chest wall in MRS breast spectra [15, 23]. When chest wall muscle is included a PCr signal a multitude greater than PME, Pi, or PDE is to be expected [15]. A relative low PCr signal is, therefore, considered a marker of good localization.

In all three metabolic ratios variations between the volunteers as well as between phases of the menstrual cycle were observed, however, also with larger standard deviations caused by relatively increased system noise when compared to the group analysis. Theoretically, an increase of PME/PDE ratio could be expected in the luteal phase. During the luteal phase progesterone levels are high, resulting in more proliferative activity, which is associated with a rise in phosphomonoesters [16, 17, 27]. On the other hand, apoptotic figures are frequently seen during the luteal phase as well [16], possibly counteracting the effect of proliferation on the PME/PDE ratio, as cell breakdown is associated with an increase in phosphodiesterases [28]. However, the observed variation in the individual data did not show a specific pattern over the menstrual cycle.

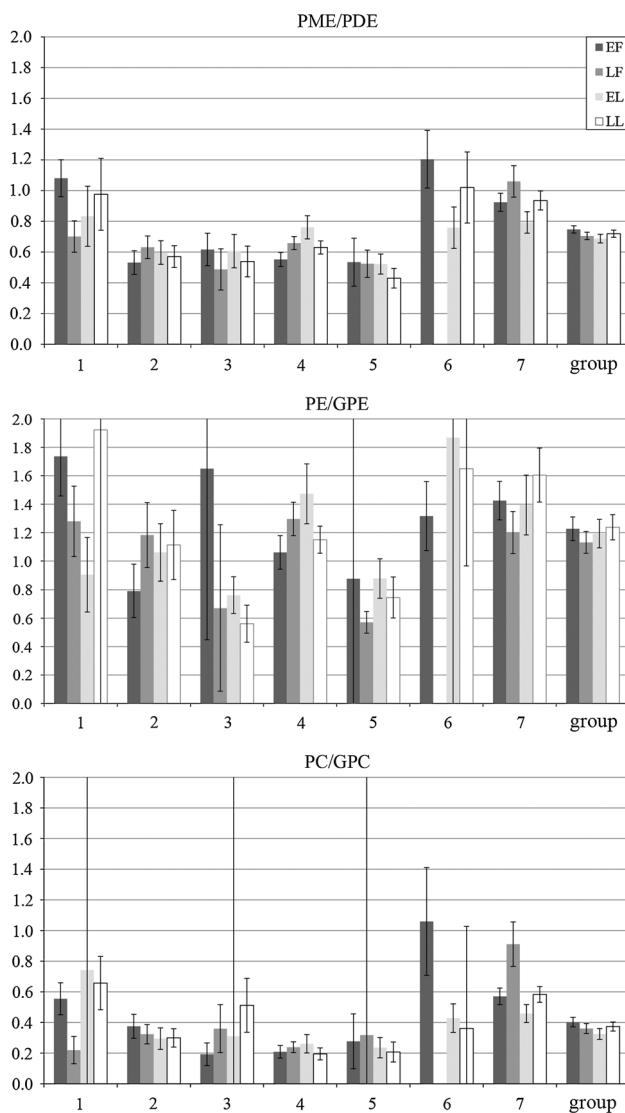


**Fig. 3** Phosphorus metabolite ratios for PME/PDE, PE/GPE, and PC/GPC over the menstrual cycle with the standard deviation caused by system noise displayed with *error bars*. The ratios shown are the individual data (1–7) and the group data (group) obtained from the T2-weighted analysis of the combined FID and multi-echo data. Note that the group results show little variation over the menstrual cycle for each ratio, which remain within standard deviations. On individual basis more variation is observed, however, without a specific pattern over the menstrual cycle

Technical aspects may also have played a role in the inter-individual variation. For instance, differences in the distribution of glandular versus lipid tissue throughout the breast result in differences in magnetic field distortions. These lead to differences in spectral line widths, which cause a reduction in SNR and more overlap between resonances, and with that to more uncertainty in the results. Also, the reproducibility of the examinations might have played a role. There are only few data on the reproducibility of  $^{31}\text{P}$  MRS(I) examinations in the breast. The data

that are available suggest a 6 % variation of total phosphate signal in patients that are examined on different days [11]. The effects on metabolic ratios are not described in that work. It would be of great value to determine the reproducibility of  $^{31}\text{P}$  MRS examinations, especially the precision. That way changes in  $^{31}\text{P}$  MRS results obtained in longitudinal patient studies can be ascribed to either disease or therapy related changes, or to the measurements' variance.

Knowing that the menstrual cycle may influence the individuals' results in different phases of the menstrual cycle, the metabolic ratios may still be used as a follow-up marker in breast cancer patients to monitor treatment efficacy. Particularly, when using a bilateral setup, the results of the contralateral breast may be used as an intra-individual reference measurement. In this study a unilateral breast coil was used. However, the first bilateral breast setups for 7 T have recently been presented [29, 30], in which double-tuning could be incorporated.

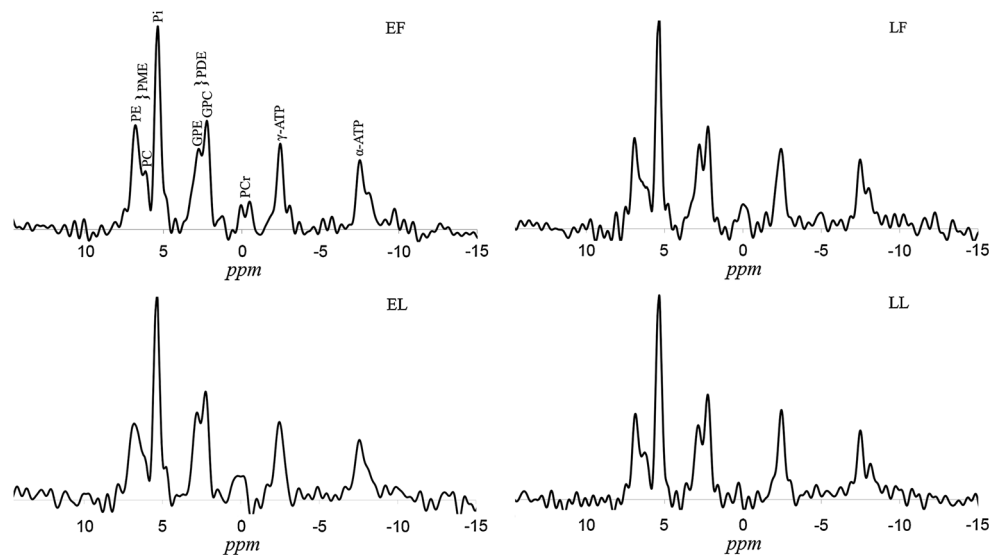
Other MR spectroscopy methods that are of interest for their value in breast cancer diagnosis or monitoring have similarly evaluated the influence of the menstrual cycle on measurement results. For instance,  $^1\text{H}$  MRS has been used to measure the lipid composition and water–fat ratio at 1.5 and 4 T, respectively [31, 32]. Both showed to be significantly influenced by the menstrual cycle, implying that menstrual cycle status is important to take into account and correct for in a patient population when using these methods. In contrast, our current study shows that the used  $^{31}\text{P}$  MRSI sequence can be applied independent of menstrual cycle status, which is favorable in a clinical setting.

T2 relaxation times were calculated to account for when using the multi-echo data to maximize the SNR. To accurately determine the T2 relaxation times all data were pooled over the volunteers and time points, assuming that T2 values do not change over the menstrual cycle. In the calculations the PDEs showed to have a much shorter T2 relaxation time than the PMEs. That could possibly lead to misinterpretation of the multi-echo data when not compensating for this difference.

T1 relaxation times were not accounted for in the analysis. This means the results are reproducible when using a TR of 6 s; however, when using different repetition times a weighting factor has to be applied on the ratios.

For our study purpose a large voxel size was used, with a spatial resolution of  $40 \times 20 \times 40 \text{ mm}^3$  (Fig. 1), combined with Hamming filtering of the data in the spatial domain, which lead to sufficient signal in almost all cases to assess all metabolic ratios. In clinical practice, however, a smaller voxel size will be mandatory, and all the SNR available from a multi-echo sequence will be needed. Still, one of the volunteers' examinations did not show enough signal from the phosphorus resonances to be included in

**Fig. 4**  $^{31}\text{P}$  MR spectra analyzed on group level, using the FID data, for each phase of the menstrual cycle; the early follicular phase (EF), late follicular phase (LF), early luteal phase (EL), and late luteal phase (LL)



the analyses. If only a small amount of glandular tissue is present, or heterogeneously spread throughout the breast, the signals can possibly not exceed the noise level. In this one particular case, combined with a sub-optimal shim setting, it led to insufficient SNR to analyze the peak integrals. Research has shown that breast cancer has much higher PME signals than normal breast tissue because of an increased phospholipid membrane anabolism [11]. PME signals have been reported to be about three times as high in breast cancer compared to benign tumors [33, 34]. Therefore, in case of the presence of a malignancy it is expected that signals will sufficiently exceed noise level even if a smaller voxel size is used.

A limitation of our study is that the menstrual cycle status was assessed per questionnaire and no serum estrogen and progesterone levels were measured to verify the cycle phase. We did only include females with regular menstrual cycles to optimally determine the menstrual cycle phase without having to take a blood sample. However, this does mean that possible anovulatory cycles were not detected, which are reported to occur in up to 14 % of healthy regular menstruating women [35].

Another limitation is that reported metabolite ratios are obtained in premenopausal women while the majority of breast cancer patients are postmenopausal. However, it has been shown that in the assessment of relative peak areas of PME, PDE, and PCr there is only a significant difference in the PCr peak between premenopausal and postmenopausal women [23]. This is probably due to breast size, because the observable PCr originated from the pectoral muscles [14]. Those data, therefore, do imply that our obtained metabolic ratios apply in postmenopausal women as well.

In conclusion, phosphorus metabolic ratios assessed using multi-echo  $^{31}\text{P}$  MRS examinations during the menstrual cycle do not show a variation on group level. On

individual basis more variation is observed, although without a specific pattern or statistical significance due to the uncertainty of the  $^{31}\text{P}$  MRS measurements in individual subjects. Therefore, without significantly affecting the results of the phosphorus metabolic ratios,  $^{31}\text{P}$  MRS examinations can be performed independent of menstrual cycle status.

**Acknowledgments** None.

**Conflict of interest** The authors declare that they have no conflict of interest.

## References

- Jemal A, Bray F, Center MM, Ferlay J, Ward E, Forman D (2011) Global cancer statistics. *CA Cancer J Clin* 61:69–90
- Mann RM, Kuhl CK, Kinkel K, Boetes C (2008) Breast MRI: guidelines from the European Society of Breast Imaging. *Eur Radiol* 18:1307–1318
- Yeh ED (2010) Breast magnetic resonance imaging: current clinical indications. *Magn Reson Imaging Clin N Am* 18:155–169
- Peters NHGM, Borel Rinkes IHM, Zuithoff NPA, Mali WPTM, Moons KGM, Peeters PHM (2008) Meta-analysis of MR imaging in the diagnosis of breast lesions. *Radiology* 246:116–124
- Loo CE, Straver ME, Rodenhuis S, Muller SH, Wesseling J, Vrancken Peeters MJTFD, Gilhuijs KGA (2011) Magnetic resonance imaging response monitoring of breast cancer during neoadjuvant chemotherapy: relevance of breast cancer subtype. *J Clin Oncol* 29:660–666
- Begley JKP, Redpath TW, Bolan PJ, Gilbert FJ (2012) In vivo proton magnetic resonance spectroscopy of breast cancer: a review of the literature. *Breast Cancer Res* 14:207
- Haddadin IS, McIntosh A, Meisamy S, Corum C, Styczynski Snyder AL, Powell NJ, Nelson MT, Yee D, Garwood M, Bolan PJ (2009) Metabolite quantification and high-field MRS in breast cancer. *NMR Biomed* 22:65–76
- Bolan PJ, Nelson MT, Yee D, Garwood M (2005) Imaging in breast cancer: magnetic resonance spectroscopy. *Breast Cancer Res* 7:149–152. doi:10.1002/nbm.1217

9. Podo F (1999) Tumour phospholipid metabolism. *NMR Biomed* 12:413–439
10. Sijens PE, Wijrdeman HK, Moerland MA, Bakker CJ, Vermeulen JW, Luyten PR (1988) Human breast cancer in vivo: H-1 and P-31 MR spectroscopy at 1.5 T. *Radiology* 169:615–620
11. Leach MO, Verrill M, Glaholm J, Smith TAD, Collins DJ, Payne GS, Sharp JC, Ronen SM, McCready VR, Powles TJ, Smith IE (1998) Measurements of human breast cancer using magnetic resonance spectroscopy: a review of clinical measurements and a report of localized <sup>31</sup>P measurements of response to treatment. *NMR Biomed* 11:314–340
12. Moestue SA, Giskeødegård GF, Cao MD, Bathen TF, Gribbestad IS (2012) Glycerophosphocholine (GPC) is a poorly understood biomarker in breast cancer. *Proc Natl Acad Sci USA* 109:E2506
13. Klomp DWJ, van de Bank BL, Raaijmakers A, Korteweg MA, Possanzini C, Boer VO, van de Berg CA, van de Bosch MAAJ, Luijten PR (2011) <sup>31</sup>P MRSI and <sup>1</sup>H MRS at 7 T: initial results in human breast cancer. *NMR Biomed* 24:1337–1342
14. Wijnen JP, van der Kemp WJM, Luttje MP, Korteweg MA, Luijten PR, Klomp DWJ (2012) Quantitative <sup>31</sup>P magnetic resonance spectroscopy of the human breast at 7 T. *Magn Reson Med* 68:339–348
15. van der Kemp WJM, Boer VO, Luijten PR, Stehouwer BL, Veldhuis WB, Klomp DWJ (2013) Adiabatic multi-echo <sup>31</sup>P spectroscopic imaging (AMESING) at 7 T for the measurement of transverse relaxation times and regaining of sensitivity in tissues with short T<sub>2</sub>\* values. *NMR Biomed* 26:1299–1307. doi:10.1002/nbm.2952
16. Ramakrishnan R, Khan SA, Badve S (2002) Morphological changes in breast tissue with menstrual cycle. *Mod Pathol* 15:1348–1356
17. Vogel PM, Georgiade NG, Fetter BF, Vogel FS, McCarty KS Jr (1981) The correlation of histologic changes in the human breast with the menstrual cycle. *Am J Pathol* 104:23–34
18. Delille JP, Slanetz PJ, Yeh ED, Kopans DB, Garrido L (2005) Physiologic changes in breast magnetic resonance imaging during the menstrual cycle: perfusion imaging, signal enhancement, and influence of the T1 relaxation time of breast tissue. *Breast J* 11:236–241
19. Müller-Schimpfle M, Ohmenhäuser K, Stoll P, Dietz K, Claussen CD (1997) Menstrual cycle and age: influence on parenchymal contrast medium enhancement in MR imaging of the breast. *Radiology* 203:145–149
20. Kuhl CK, Bieling HB, Gieseke J, Kreft BP, Sommer T, Lutterbey G, Schild HH (1997) Healthy premenopausal breast parenchyma in dynamic contrast-enhanced MR imaging of the breast: normal contrast medium enhancement and cyclical-phase dependency. *Radiology* 203:137–144
21. Rieber A, Nüssle K, Merkle E, Kreienberg R, Tomczak R, Brambs HJ (1999) MR mammography: influence of menstrual cycle on the dynamic contrast enhancement of fibrocystic disease. *Eur Radiol* 9:1107–1112
22. Payne GS, Dowsett M, Leach MO (1994) Hormone-dependent metabolic changes in the normal breast monitored non-invasively by <sup>31</sup>P magnetic resonance (MR) spectroscopy. *The Breast* 3:20–23
23. Twelves CJ, Lowry M, Porter DA, Dobbs NA, Graves PE, Smith MA, Richards MA (1994) Phosphorus-31 metabolism of human breast: an in vivo magnetic resonance spectroscopic study at 1.5 Tesla. *Br J Radiol* 67:36–45
24. Stehouwer BL, Klomp DWJ, Korteweg MA, Verkooijen HM, Luijten PR, Mali WPTM, van den Bosch MAAJ, Veldhuis WB (2013) 7T versus 3T contrast-enhanced breast Magnetic Resonance Imaging of invasive ductal/lobular carcinoma: first clinical experience. *Magn Reson Imaging* 31:613–617
25. Naressi A, Couturier C, Devos JM, Janssen M, Mangeat C, de Beer R, Graveron-Demilly D (2001) Java-based graphical user interface for the MRUI quantitation package. *MAGMA* 12:141–152
26. Vanhamme L, van den Boogaart A, Van Huffel S (1997) Improved method for accurate and efficient quantification of MRS data with use of prior knowledge. *J Magn Reson* 129:35–43
27. Glaholm J, Leach MO, Collins DJ, Mansi J, Sharp JC, Madden A, Smith IE, McCready VR (1989) In-vivo <sup>31</sup>P magnetic resonance spectroscopy for monitoring treatment response in breast cancer. *Lancet* 1:1326–1327
28. Twelves CJ, Porter DA, Lowry M, Dobbs NA, Graves PE, Smith MA, Rubens RD, Richards MA (1994) Phosphorus-31 metabolism of post-menopausal breast cancer studied in vivo by magnetic resonance spectroscopy. *Br J Cancer* 69:1151–1156
29. Brown R, Storey P, Geppert C, McGorty KA, Leite APK, Babb J, Sodickson DK, Wiggins GC, Moy L (2013) Breast MRI at 7 Tesla with a bilateral coil and T1-weighted acquisition with robust fat suppression: image evaluation and comparison with 3 Tesla. *Eur Radiol* 23:2969–2978. doi:10.1007/s00330-013-2972-1
30. Italiaander MGM, Nijholt PJ, Kraft O, Raaijmakers A, Stehouwer BL, Luijten PR, Klomp DWJ (2012) High B1 duty cycle in bilateral breast imaging at 7T. Proceedings of the 18th Annual Meeting of ISMRM, Melbourne, Australia, 1493
31. Dzendrowskyj TE, Noyszewski EA, Beers J, Bolinger L (1997) Lipid composition changes in normal breast throughout the menstrual cycle. *MAGMA* 5:105–110
32. Sharma U, Kumar M, Sah RG, Jagannathan NR (2009) Study of normal breast tissue by in vivo volume localized proton MR spectroscopy: variation of water-fat ratio in relation to the heterogeneity of the breast and the menstrual cycle. *Magn Reson Imaging* 27:785–791
33. Degani H, Horowitz A, Itzchak Y (1986) Breast tumors: evaluation with P-31 MR spectroscopy. *Radiology* 161:53–55
34. Ng TC, Grundfest S, Vijayakumar S, Baldwin NJ, Majors AW, Karalis I, Meaney TF, Shin KH, Thomas FJ, Tubbs R (1989) Therapeutic response of breast carcinoma monitored by <sup>31</sup>P MRS in situ. *Magn Reson Med* 10:125–134
35. Filiberto AC, Mumford SL, Pollack AZ, Zhang C, Yeung EH, Schliep KC, Perkins NJ, Wactawski-Wende J, Schisterman EF (2013) Usual dietary isoflavone intake and reproductive function across the menstrual cycle. *Fertil Steril* 100:1727–1734